Geodetic and paleogeodetic resolution of locked patches on the Sunda megathrust, offshore Sumatra

Mohamed Chlieh, Jean-Philippe Avouac, Kerry Sieh, Danny H. Natawidjaja, John Galetzka,
Tectonic Observatory, Caltech, Pasadena, CA
Research Center for Geotechnology, Bandung, Indonesia

Geodetic and paleogeodetic measurements of strain above the Sumatran portion of the Sunda subduction zone reveal a heterogeneous pattern of coupling along the subduction megathrust. Annual banding in coral heads provides vertical rates of deformation spanning the last half of the 20th century and repeated GPS surveys between 1991 and 2004 and continuous measurements at GPS stations operated since 2002 provide horizontal velocities. The area of the plate interface within which the coupling is high is only ~75 km wide near the Equator but increases to ~175 km farther south. Major sections of this Locked Fault Zone (LFZ) coincide with the rupture areas of major Mw>8.5 interplate earthquakes. The section that ruptured during the Mw 8.7 Nias earthquake of 2005 released about 2/3 of the slip deficit that had accumulated since its previous rupture in 1861. Farther south, beneath the Mentawai islands, overlapping ruptures of the LFZ produced giant earthquakes in 1797 and 1833. The accumulated slip deficit since these events is slowly reaching the amount of slip that occurred during the 1833 earthquake but already exceeds the slip that occurred during the 1797 earthquake. Thus, re-rupture of the Mentawai patch in the near future seems quite likely. In contrast, coupling is low in the Batu islands near the Equator and around Enganno island at about 5S, where only moderate earthquakes have occurred in the past two centuries. Temperature might influence the mode of slip along the plate interface, through its effect on the rheology of sediments at the plate interface. Other influences, such as structures on the subducting plate, could also play a role. In particular, subduction of the Investigator Fracture Zone near the Equator coincides with the relatively low coupling there.

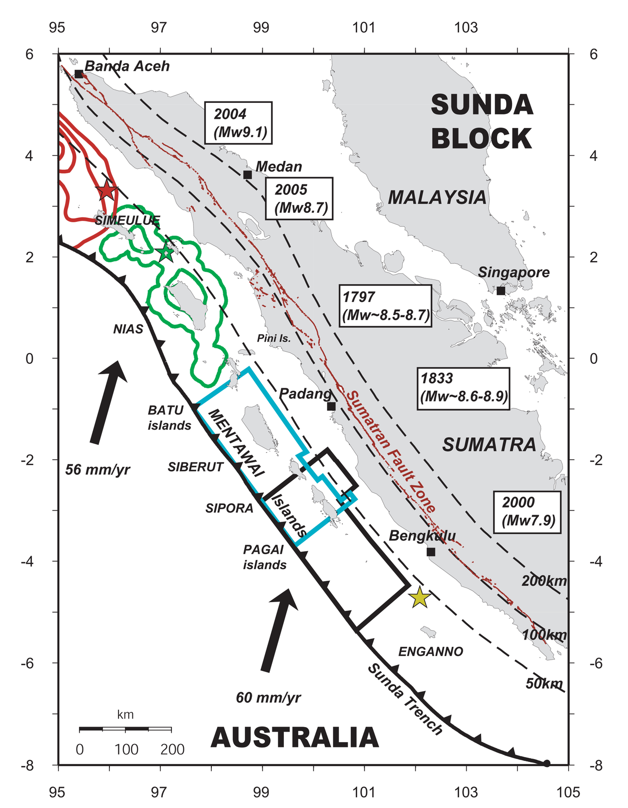

Seismo-tectonic setting of the Mentawai segment along Sumatra subduction zone with location of rupture area of M>8 earthquakes since 1700. The Mw8.7 1861 Nias earthquake that has broke a similar segment than the Nias 2005 earthquake is not reported [Briggs et al. 2006; Newcomb and McCann 1987]. Rupture area of the 2004 Sumatra-Andaman (red) and 2005 Nias earthquake (green) are represented by their 5m coseismic slip contours [Chlieh et al. 2006; Hsu et al. 2006]. Ruptures of the 1797 (blue) and 1833 (black) earthquakes show the elastic dislocation models of coral records of co-seismic uplift [Natawidjaja et al. 2006a]. It is not clear whether the 1833 rupture ends north, or extends south of Enganno island. Iso-depth contours 50km, 100km and 200km (dashed lines) of the megathrust interface are from [Gudmundsson and Sambridge 1998].

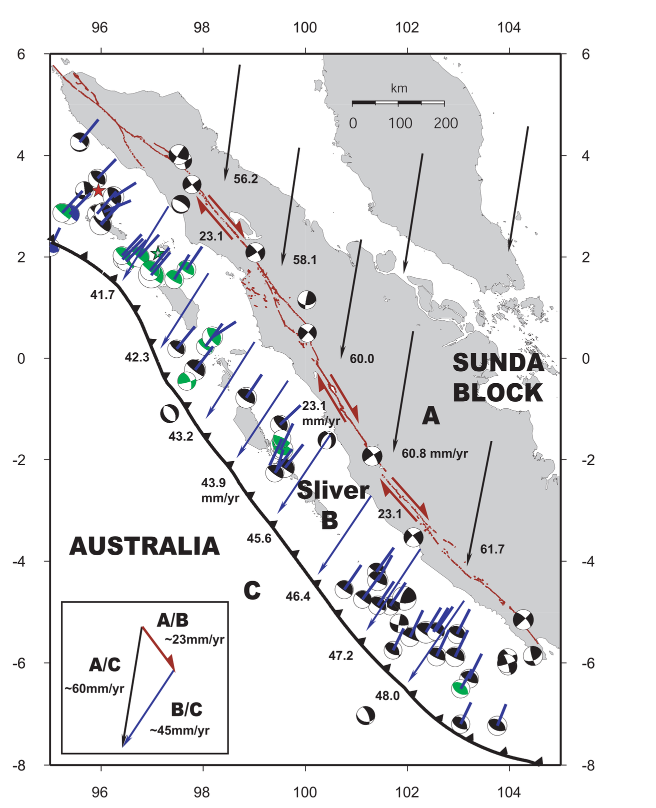

Secular motion of the Sumatra forearc Sliver (B) relative to Australia (C). Plate motion of Sunda, A (black arrows) relative to Australia determined from [Bock et al. 2003] (see parameters in Table 1) and from the Sumatra forearc sliver, B (blue arrows), relative Australia, C. Focal mechanisms of Mw>6 earthquakes between 1976 and June 2005, are from the Harvard centroid moment tensor (CMT) catalogue. CMT after the March 2005 Nias earthquake are in green. Assuming that the Sumatran Fault Zone is purely strike-slip and that the slip vectors of interplate earthquakes is parallel to the long term slip along the plate interface, the Sunda/Australia oblique convergence (black arrow in inset) is partitioned into ~23mm/yr strike-slip motion along the Sumatran Fault Zone (red arrows in inset) and about 42-

FORWARD MODELS AND INVERSION

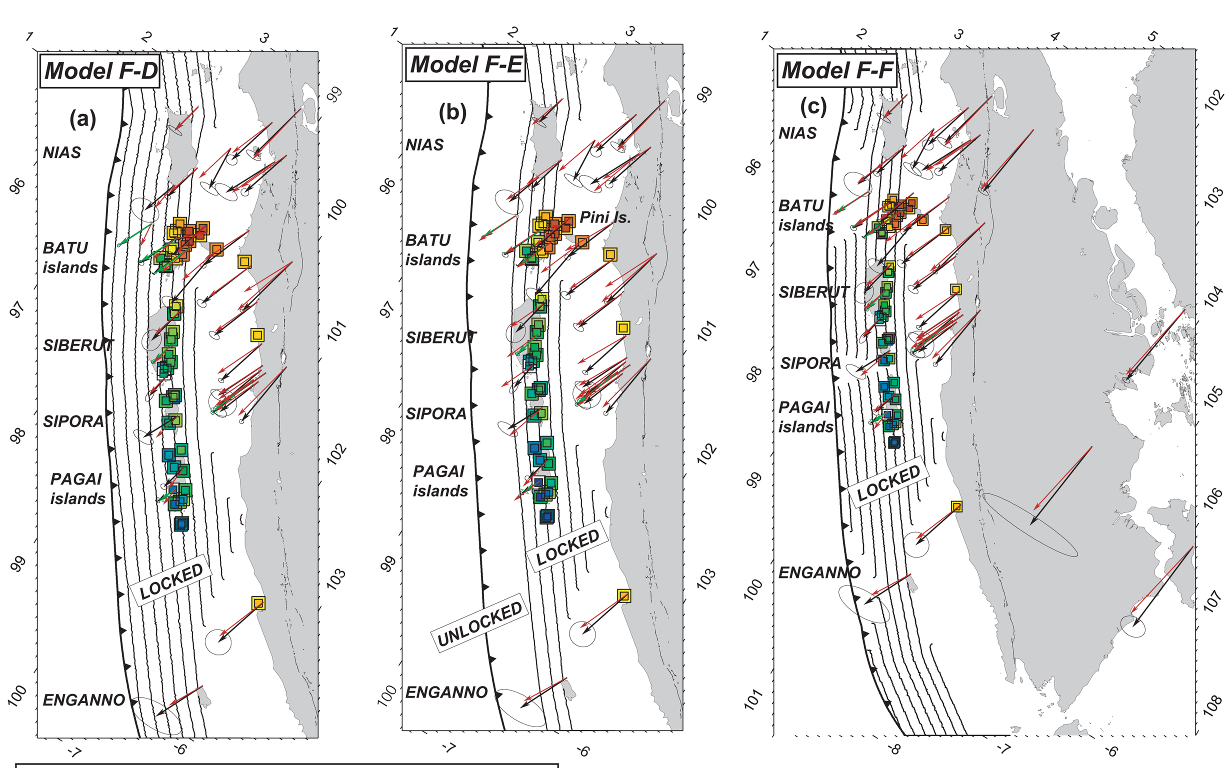

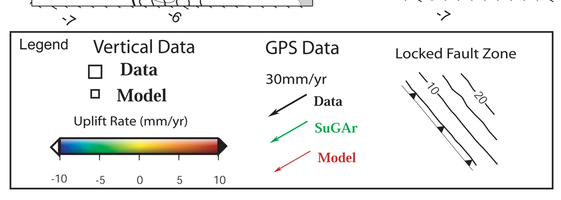

Three-dimensional back-slip model with variable widths of locked fault zone. The interseismic LFZ of the megathrust interface is represented each 5km-depth contour lines. Three tests are done with different hypothesis on the distance of the LFZ updip limit to the trench, (a) the LFZ reaches the trench everywhere (Model F-D), (b) it is at 50km from the trench everywhere (Model F-E) and (c) it is at variable distance from the trench (Model F-F). The predicted GPS velocities are in red and the observed in black (Bock et al. 2003) and green (SuGAr data). The predicted vertical rates are represented by small squares inside the observed vertical rates (big squar), all scaled using the same color bar.

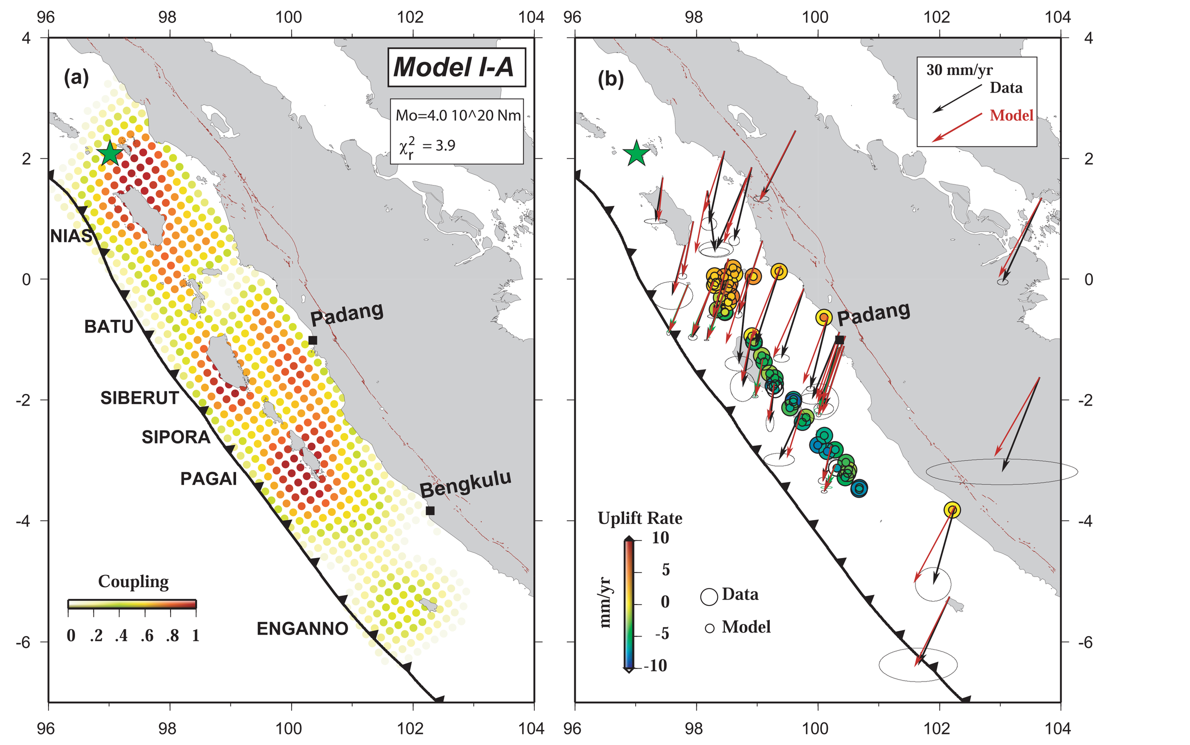

Inversion of the coral and GPS data weighted by their 1-sigma uncertainties. (a) Coupling distribution on the megathrust interface of model I-A (Table 7). Fully coupled areas are in red color and fully creeping area are in white. The gradual decoupling is shown by the color bar. The accumulated moment deficit rate of that inversion is 4.0 x 1020 Nm/yr. (b) Predicted displacements are represented by red vectors for the GPS and by small circles for the data. The reduced Ki^2 of this model is 3.9.

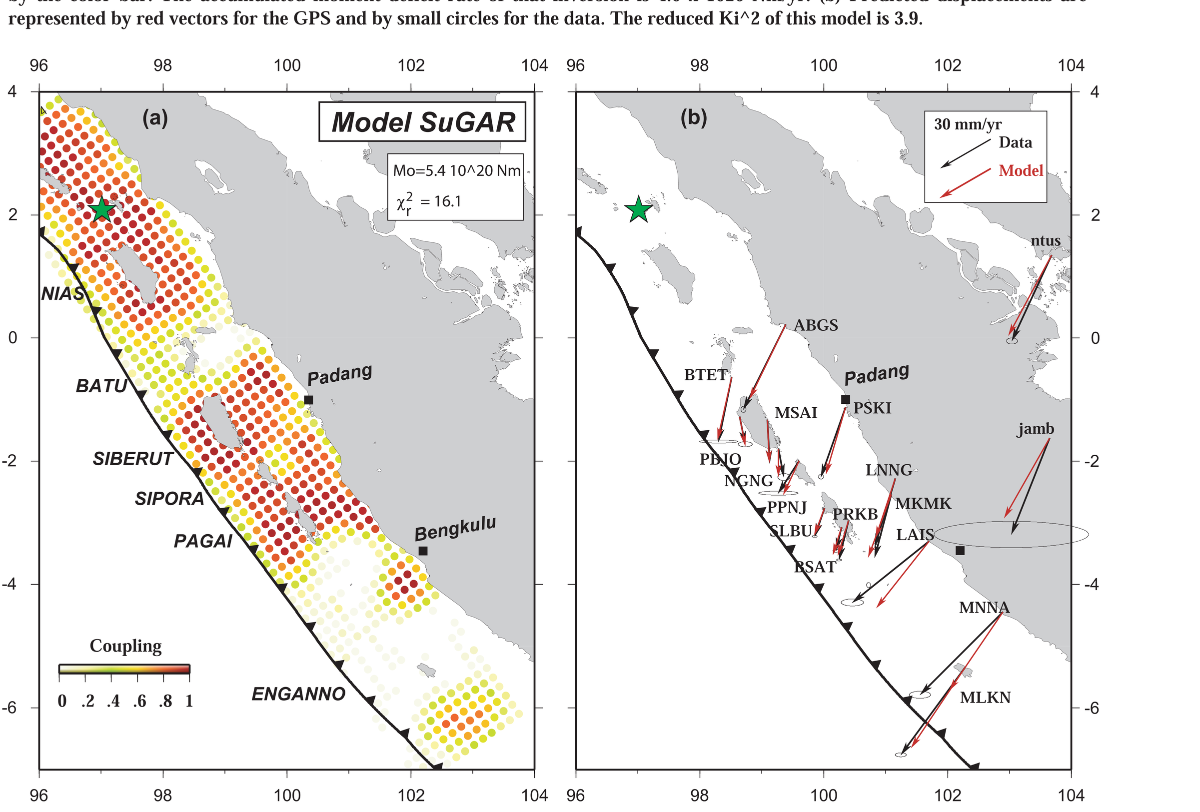

Inversion of the SuGAR Continuous GPS data weighted by their 1-sigma uncertainties. The velocities of all CGPS stations were determined from the time series processed by SOPAC. To reduce deformation related to the postseismic relaxation of the March 2005 Nias earthquake, the velocities were determined for the time-window June 2005 (3 month after the Nias earthquake) to September 2006. (a) Coupling distribution on the megathrust interface. That model suggests that the megathrust portion south of the Pagai islands is creeping at the plate velocity. It confirms also that the 400 km long Siberut-Pagai segment right off-shore Padang city shows a very wide and high coupling. (b) Observed and modelled GPS velocities.

THERMAL MODELS

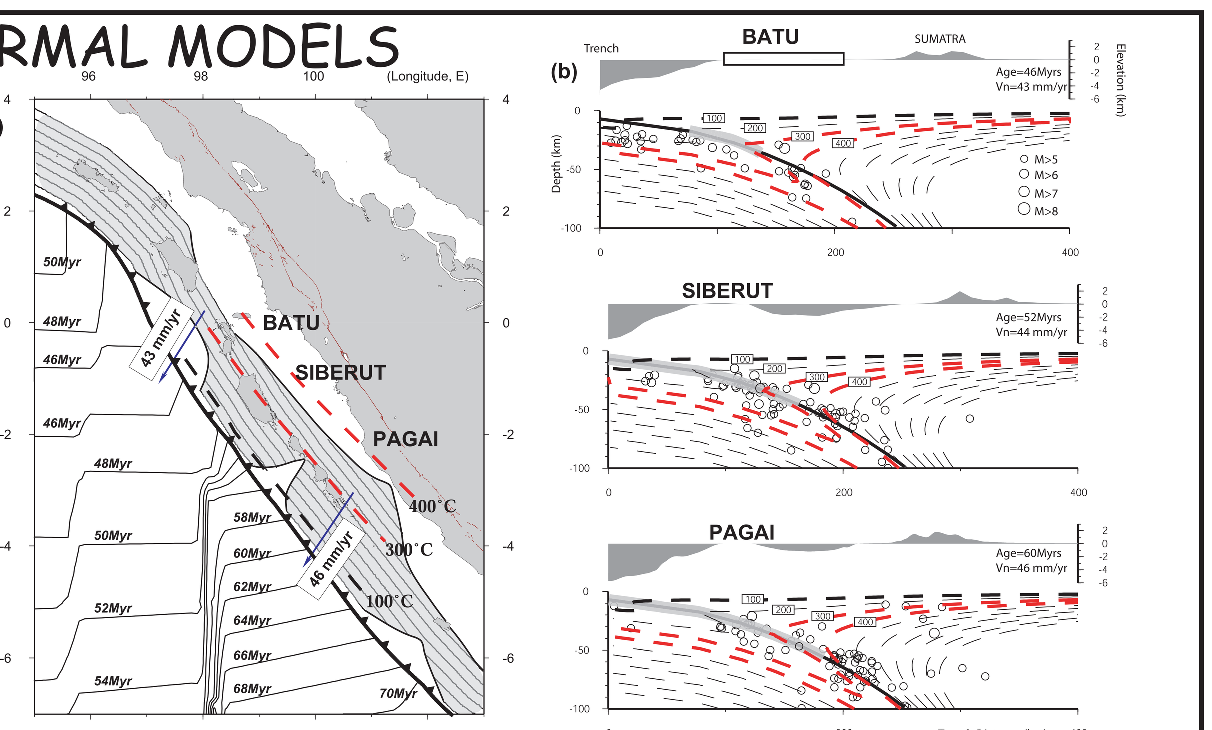

(a) Map view of the isotherms 100˚C, 300˚C and 400˚C as deduced from the thermal modelling superposed on top of the LFZ of model F-F. The lateral variations of the age of the subducting oceanic plate are indicated in Myr [Cande and Kent 1995; Gradstein et al. 1994]. (b) Topographic and steady state thermal structure of the meagthrust interface for three trench-normal sections across the Batu, Siberut and Pagai islands. The slab interface is drawn using the background relocated seismicity catalogue of [Engdhal et al. 1998]. The LFZ of the meagthrust interface deduced from Model F-F are reported in grey. Isotherms are computed from analytical expression of the steady state thermal structure model proposed by {Royden, 1993 #362}. The model accounts for conduction, advection, a shear heating of 40 mW/m2 and upper plate radiogenic heat production of 0.4 mW/m3. The two parameters varying between profiles are the age and the normal convergence velocity of the subducting plate . On each profile, the downdip end of the

PALEOGEODETIC AND GEODETIC DATA

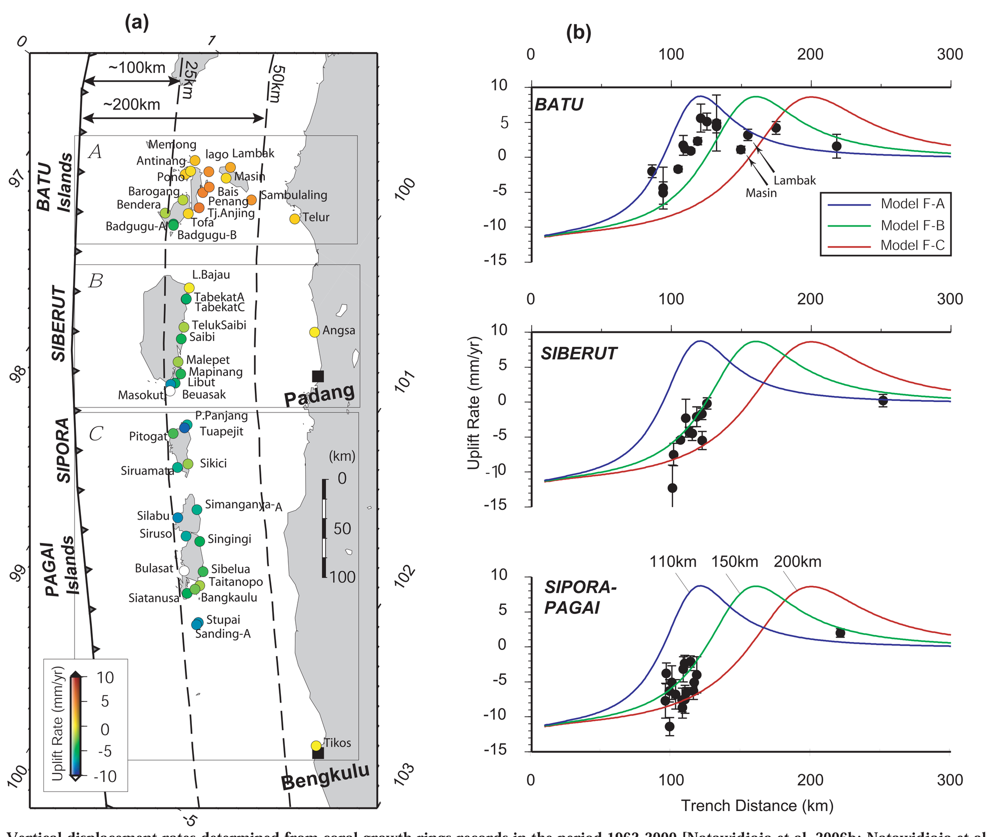

Vertical displacement rates determined from coral growth rings records in the period 1962-2000 [Natawidjaja et al. 2006b; Natawidjaja et al. 2004] in map view and along sections normal to the trench. Boxes indicate the swath corresponding to each section. The origin of horizontal axis on each section is at the trench. The forearc islands are dominantly subsiding as expected if this pattern is consistent with the shallow portion of the plate interface being locked to some degree during this interseismic period. For reference, the continuous lines in the sections show the predicted uplift rates computed assuming that the plate interface is fully locked from the trench to a depth of 30, 40, or 50km, corresponding to a increasing width of the LFZ of ~110km (blue), 150km (green) and 200km (red). Subsidence rates generally increase southward along strike suggesting the LFZ is narrower in the Batu islands area near the Equator.

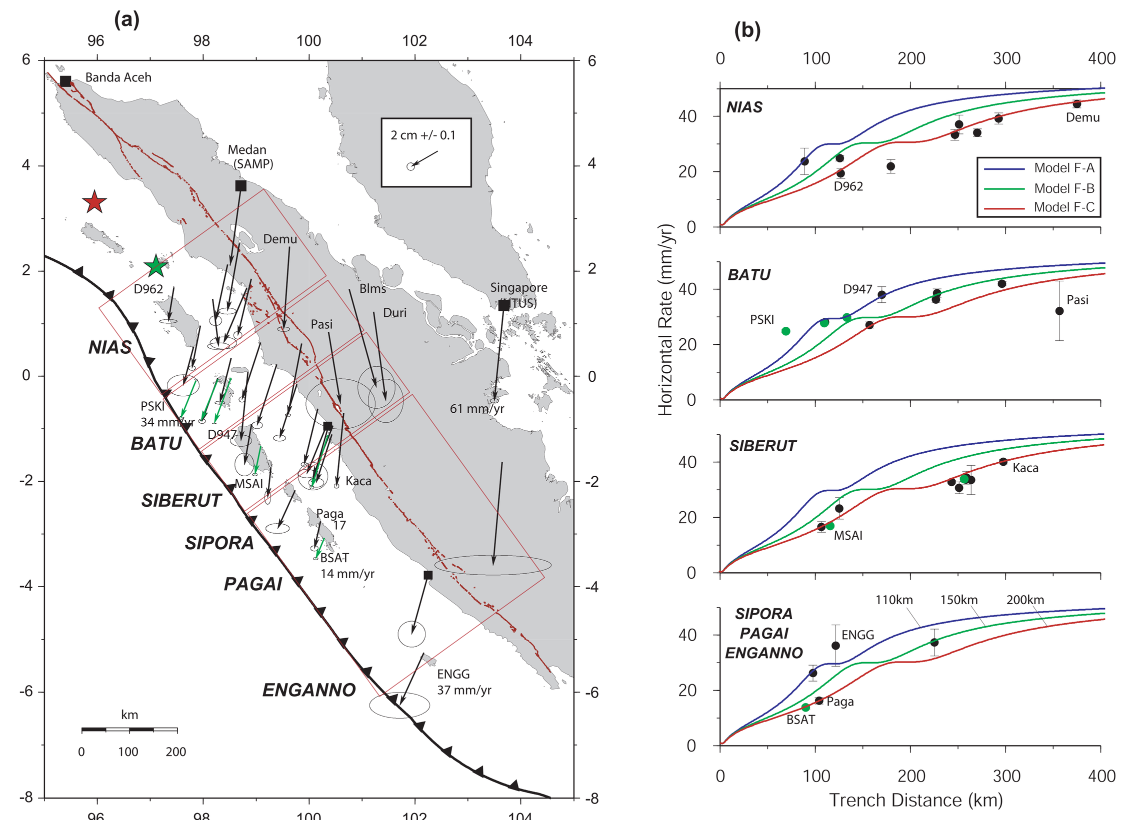

Horizontal velocities relative to Australia, as defined by the plate motion of Australia relative to ITRF200 of Bock et al. (2003), at campaign sites (black arrows) and at the Continuous GPS station of the Sumatra Geodetic Array, SuGAr, (green arrows). Ellipses show uncertainties at the 1-? confidence level (Tables 3 and 4). Plots on the sides show the trench normal horizontal velocities along various sections. The boxes on the map view indicate the swaths corresponding to each section. The origin of horizontal axis on each section is at the trench. Velocities decrease from the Sunda Shelf toward the trench from 60mm/yr to 14mm/yr. Predictions from model F-A, F-B, and F-C corresponding to a Locked fault Zone width of respectively 110, 150 and 200km are shown for comparison (Table 5).

Locked Fault Zone Vs 1797, 1833, 2005 Giant earthquakes

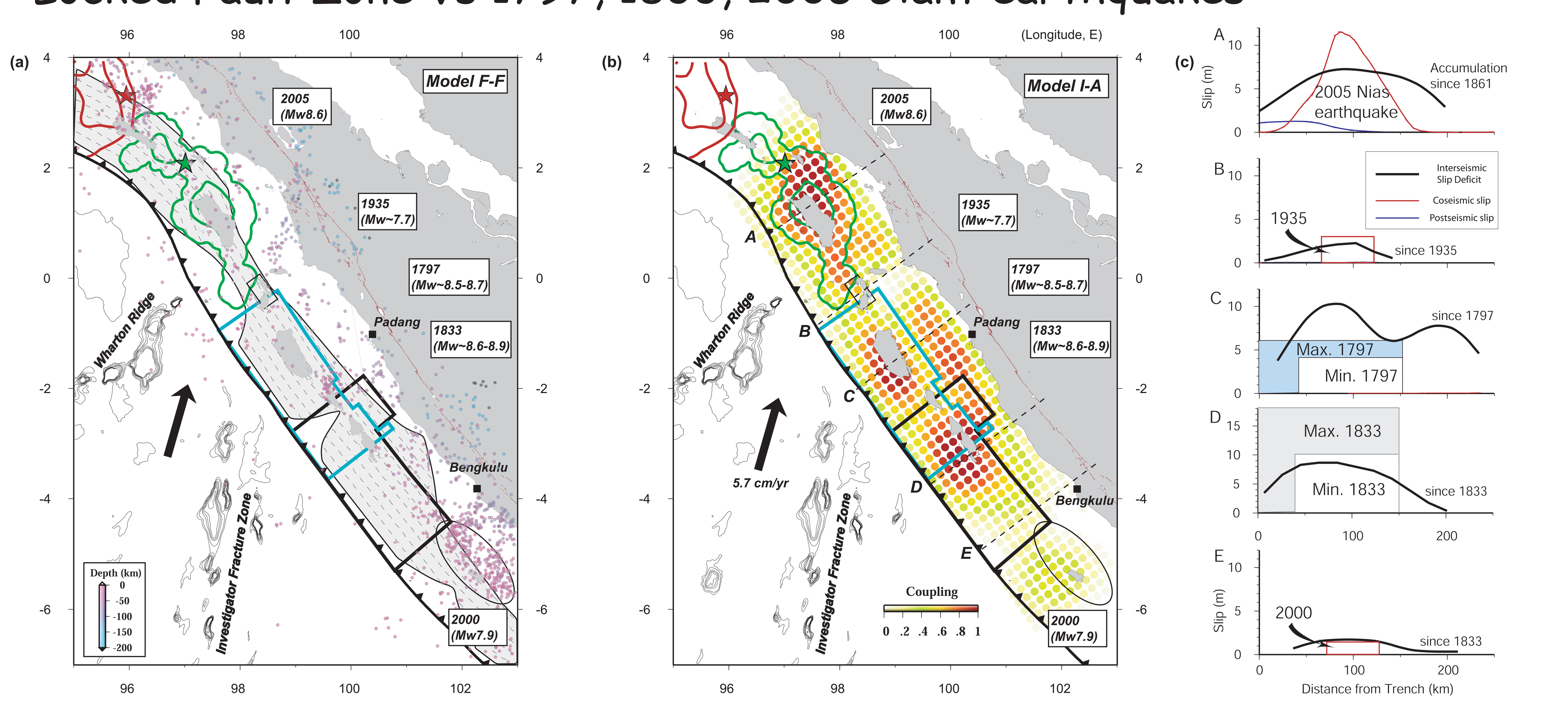

(a) LFZ of model F-F. Below the Batu Islands where the LFZ is narrow, only large earthquake (Mw>7-7.5) happened since below the Siberut and Pagai Islands where the LFZ is wide, giant earthquakes (Mw>8-9) occurred. Background seismicity from [Engdhal et al. 1998] traces relatively well the downdip end of the Locked Fault Zone. The embayment of the LFZ in the Batu could be related to the subducting fossil Investigator Fracture Zone. (b) LFZ of model A-I is shown. Note the remarkable coincidence of the high coupling area (orange-red dots) with the 5m coseismic slip contours of the 2005 Nias earthquake. The 1797 and 1833 ruptures from Natawidjaja et al. 2006 are also well centred on highly coupled asperities. The southernmost rupture

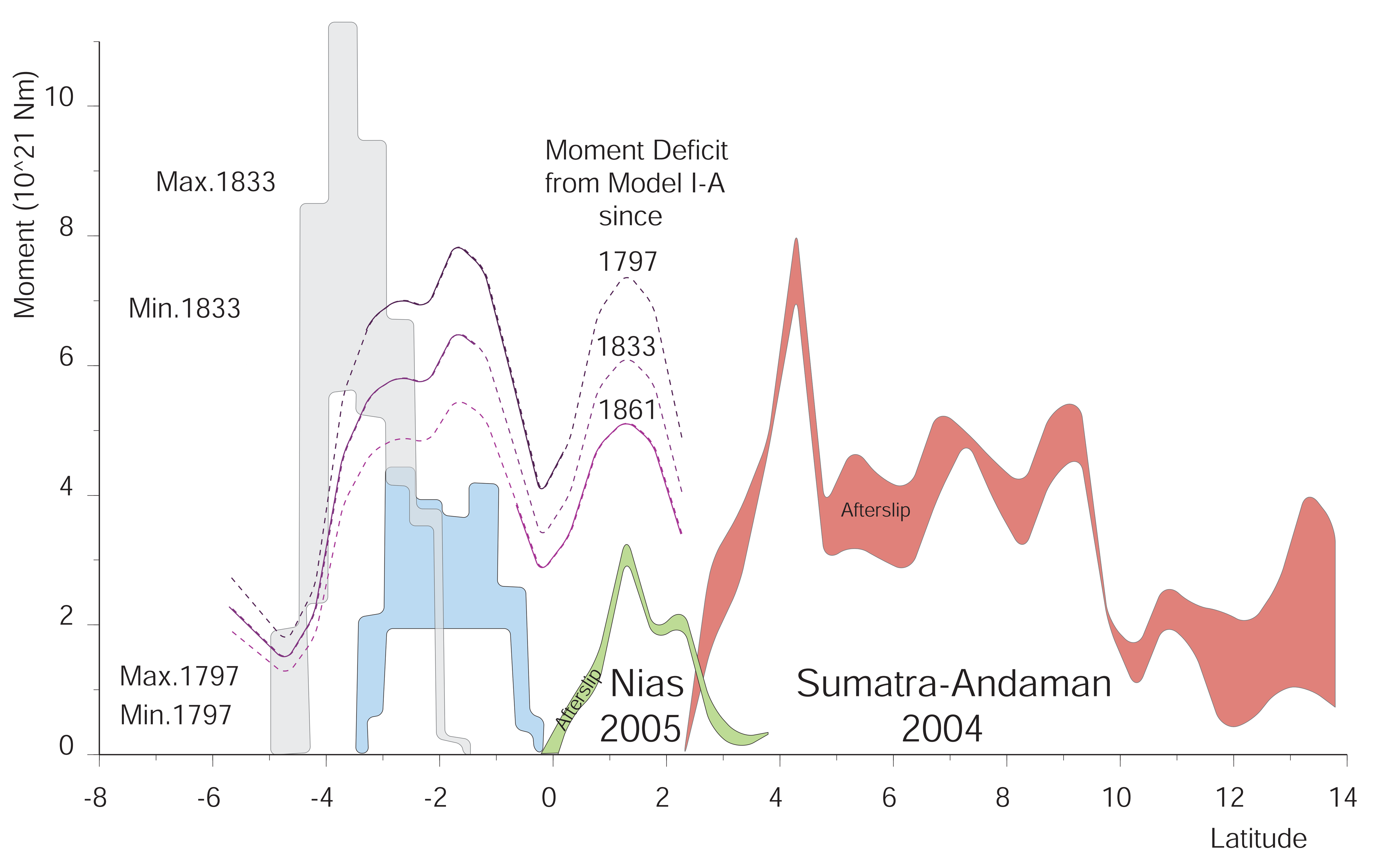

Latitudinal variations of scalar moments as function of latitude for the 2004 Sumatra-Andaman earthquake [Chlieh et al. 2006], the 2005 Nias earthquake [Konca et al. 2006], and 1797 and 1833 Mentawai earthquakes [Natawidjaja et al. 2006a]. For comparison, the cumulated interseismic deduced since 1797, 1833 and 1861 are shown from the prediction of model I-A